Molecular Dynamics Calculation of Thermal Conductivity of Graphene Nanoribbons

Jiuning Hu[1], Xiulin Ruan[2], Zhigang Jiang[3] and Yong P. Chen[4]

[1]School of Electrical and Computer Engineering and Birck Nanotechnology Center, Purdue University, West Lafayette, Indiana 47907, USA
[2]School of Mechanical Engineering and Birck Nanotechnology Center, Purdue University, West Lafayette, Indiana 47907, USA
[3]School of physics, Georgia Institute of Technology, Atlanta, Georgia 30332, USA
[4]Department of physics, School of Electrical and Computer Engineering and Birck Nanotechnology Center, Purdue University, West Lafayette, Indiana 47907, USA

Abstract. We have used classical molecular dynamics based on the Brenner potential to calculate the thermal conductivity of rectangular graphene nanoribbons up to 30 nm long. We have employed the Debye model to make the quantum correction of the classical molecular dynamics temperature. The calculated thermal conductivity is on the similar order of magnitude of the experimentally measured value for graphene. The edge chirality dependence of thermal conductivity shows that nanoribbons with zigzag long edges have larger thermal conductivity than that of nanoribbons with armchair edges. Our investigation of the size dependence of the thermal conductivity indicates that the calculated value is limited by the finite length of nanoribbons.

Keywords: Graphene nanoribbons, molecular dynamics, thermal conductivity, quantum correction, chirality dependence, size dependence.
PACS: 62.30.+d, 63.20.-e, 63.22.-m.

INTRODUCTION

Graphene, a two dimensional monolayer of graphite with sp^2 carbon bonds, has drawn much attention due to its extraordinary electronic properties [1-5]. Graphene nanoribbons (GNRs), strips of graphene with few or few tens of nm in size, have been considered as excellent candidates of future carbon-based nanoelectronics. For example, it has been shown that many electronic properties of GNRs may be tuned by their width or edge structures [6-9]. Graphene also has exceptional thermal properties with fundamental and practical importance. Recently, it has been experimentally shown [10, 11] that graphene has an unusual high thermal conductivity, comparable or possibly even superior to those well-known materials with high thermal conductivity, such as carbon nanotubes (CNTs) [12, 13] and graphite [14] (ab-plane). This will enable us to use graphene nanostructures for nanoscale thermal management. In this work, we have used classical molecular dynamics to simulate thermal transport in GNRs of few nanometers in size. We have found that the thermal conductivity of GNRs depends on the edge-chirality.

We also studied the size effect of GNRs on their thermal conductivity. In the calculation, we have taken the quantum effect into account by considering the occupation number and density of states (DOS) of phonons. GNRs can be potentially used in nanoscale thermal management such as on-chip cooling and energy conversion.

MOLECULAR DYNAMICS

In our simulation, we have used classical molecular dynamics (MD) based on the Brenner potential [15]. The Brenner potential is a many-body potential for hydrocarbon systems that considers the coordination number of each atom. The anharmonic effects, causing the phonon scattering and consequently leading to finite value of thermal conductivity, have been automatically embedded in the Brenner potential. The carbon atoms denoted by triangles in Figure 1 at the two ends of the GNR are placed in the Nosé-Hoover thermostats [16, 17] (obeying equation (1)) at temperatures T_L (left-pointing triangles) and T_R (right-pointing triangles) respectively. The absolute value of

the temperature difference is $\Delta T = |T_L - T_R|$. The equations of motion for atoms in either the left or right Nosé-Hoover thermostat are:

$$\frac{d}{dt} p_i = F_i - \gamma p_i,$$

$$\frac{d}{dt} \gamma = \frac{1}{\tau^2}\left[\frac{T(t)}{T_0} - 1\right], T(t) = \frac{2}{3Nk_B}\sum_i \frac{p_i^2}{2m} \quad (1)$$

where the subscript i runs over all the atoms in the thermostat, p_i is the momentum of the i-th atom, F_i is the total force acting on the i-th atom, γ and τ are the dynamic parameter and relaxation time of the thermostat, T is the instant temperature of the thermostat at time t, T_0 ($=T_L$ or T_R) is the set temperature of the thermostat, N is the number of atoms in the thermostat, k_B is the Boltzmann constant and m is the mass of the carbon atom. We used the 3rd-order prediction-correction method to integrate these equations of motion. The time step is 0.5 fs and the simulation is run for 10^7 time steps (the total MD time is 5 ns). The relaxation time τ is 1 ps. Typically, $T(t)$ can stabilize around the set value T_0 after about 0.5 ns. We did the time averaging of the temperature and heat current from 2.5 ns to 5 ns. The heat current injected to the thermostat is given by [18]

$$J = \sum_i \left(-\gamma p_i\right) p_i / m = -3\gamma Nk_B T(t) \quad (2)$$

In Figure 1, the atoms denoted with squares at the ends are fixed to avoid the spurious global rotation of the GNRs in the simulation [19]. The atoms denoted with circles obey the Newton's law of motion of equation (3):

$$\frac{d}{dt} p_j = F_j \quad (3)$$

where j runs over all atoms neither fixed nor in any thermostats.
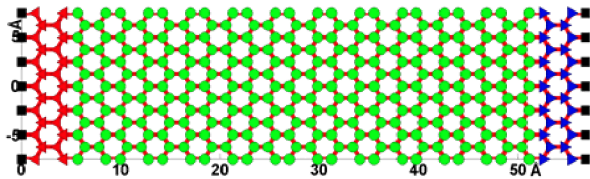

FIGURE 1. Rectangular armchair GNR of 1.5 nm × 5.7 nm used in this study.

Thermal conductivity is ideally defined as the limit $\kappa = \lim_{\Delta T \to 0} Jd/(\Delta Twh)$ according to Fourier's law, where d, w and h (=0.335 nm) are the length, width and thickness of the GNR respectively. In non-equilibrium MD simulation, however, this mathematical limit cannot be realized due to the fluctuations in both the temperature difference ΔT and the resulting heat current J. If ΔT is too small to dominate its fluctuations, the calculation of thermal conductivity could become problematic. To address this problem, we defined $\alpha = \Delta T/(2T)$ where $T = (T_L + T_R)/2$ and examined the thermal current as a function of α for the GNR in Figure 1. The result is shown in Figure 2. We found that it is still in linear response region up to α=10%, so we set α=10% in all following simulations. At steady state, in principle $J_L + J_R = 0$ because there is no energy accumulation. However, $J_L + J_R$ slightly fluctuates around zero. Therefore, the heat current and its error are defined as $J = (J_L - J_R)/2$ and $\Delta J = |J_L + J_R|/2$ (corresponding to the error in the thermal conductivity $\Delta\kappa = \Delta Jd/(\Delta Twh)$).
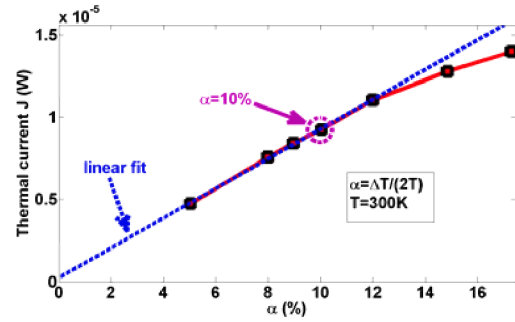

FIGURE 2. Thermal current versus α (solid line) and its linear fit (dashed line).

We corrected the temperature calculated from equation (1) by considering the phonon occupation number and DOS of 2-dimensional graphene lattice. We only consider phonons of three acoustic branches and assume linear dispersion with phonon sound velocities v_{LA}=19.5 km/s, v_{TA}=12.2 km/s and v_{ZA}=1.59 km/s. Therefore, the phonon DOS is $D(\omega) = 3\omega/(2\pi nv^2)$, where v is the effective phonon sound velocity satisfying $3v^{-2} = v_{LA}^{-2} + v_{TA}^{-2} + v_{ZA}^{-2}$ and n is the number of carbon atoms in unit area of graphene. The phonon energy per carbon atom at temperature T from the Debye model should equal to the kinetic energy per carbon atom $3k_B T_{MD}$, i.e.,

$$\int_0^{\omega_D} D(\omega)n(\omega,T)d\omega = 3k_B T_{MD}$$

$$n(\omega,T) = \left(e^{\hbar\omega/k_B T} - 1\right)^{-1} \quad (4)$$

136

where $\omega_D = k_D v$ ($k_D = (4\pi n)^{1/2}$) is the Debye frequency, $n(\omega,T)$ is the phonon occupation number and T_{MD} is the classical MD temperature. The scheme of quantum correction of temperature can be obtained from equation (4):

$$T_{MD} = \frac{2T^3}{T_D^2} \int_0^{T_D/T} \frac{x^2}{e^x - 1} dx \qquad (5)$$

where $T_D = \hbar\omega_D/k_B$ is the Debye temperature (322 K). It is worthy to note that the zero-point-energy is not included in the phonon occupation number because the corresponding temperature is one third of the Debye temperature (107 K), which means that there is no corresponding quantum corrected temperature if the classical MD temperature is below 107 K. Figure 3 shows the difference after introducing the zero-point-energy during the quantum correction. In all of the following MD results, the temperature axis represents quantum corrected temperature.
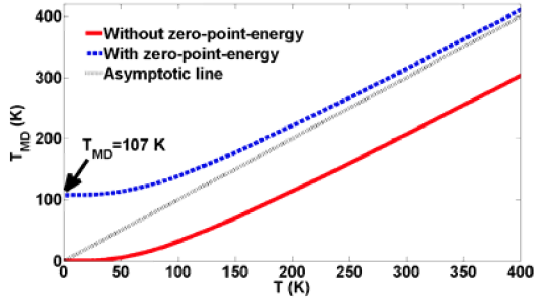

FIGURE 3. Quantum correction of the MD temperature. The solid (dashed) line is the result without (with) the zero-point-energy included. The dotted is the asymptotic line at high temperature.

RESULTS AND DISCUSSION

We have calculated the thermal conductivity of the rectangular GNR in Figure 1. The solid line in Figure 4 shows the thermal conductivity of this 5.7-nm long and 1.5-nm wide GNR as a function of temperature. The thermal conductivity is around 1700 W/m-K at 400 K (Figure 4), on the same order of magnitude with the experimental measured value (~3000-5000 W/m-K) of graphene [10, 11].

We studied the effect of the finite size of GNRs on their thermal conductivities. In Figure 4, When the length of this GNR is doubled (the width remaining unchanged), the calculated thermal conductivity almost doubles (dashed line). It is probable that our calculated thermal conductivity is limited by the finite length of GNRs, which is consistent with the large

phonon mean free path (MFP) in graphene extracted from the experiment (775 nm) [11]. The size of GNRs in this study is only up to ~30 nm. Therefore, our calculated thermal conductivity is not corresponding to the value for graphene of macroscopic size. In addition, we have also found that the calculated thermal conductivity remains nearly the same after doubling the width of GNRs (the length remains unchanged), as indicated by the dash-dotted line of Figure 4. As we see from Figure 4, the thermal conductivity monotonically increases with temperature (T), in the range we studied (180-400 K), for GNRs up to ~10 nm long. Our results are consistent with a recent theory by Nika *et al.* on small graphene flakes (e.g., 5 μm long) where the important roles of phonon scattering by graphene edges in the temperature dependence of thermal conductivity have been discussed [20].
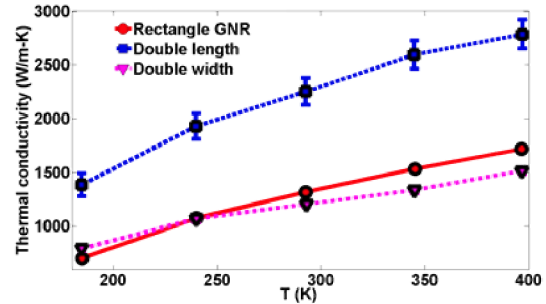

FIGURE 4. Thermal conductivity of the GNR in Figure 1(a) (solid line) and that of the GNR with double length (dashed line) and width (dash-dotted line) only.

We also investigated the thermal conductivity of rectangular GNRs with armchair or zigzag long edges. We found that the GNRs with zigzag long edges have larger thermal conductivity than GNRs with armchair long edges. Figure 5 shows the calculated thermal conductivity of GNRs with armchair (solid line) and zigzag (dashed line) long edges as a function of their length at T=400 K. The thermal conductivity of GNRs increase with their length, which is consistent with the result of Figure 4 and phonon MFP limited value of thermal conductivity.
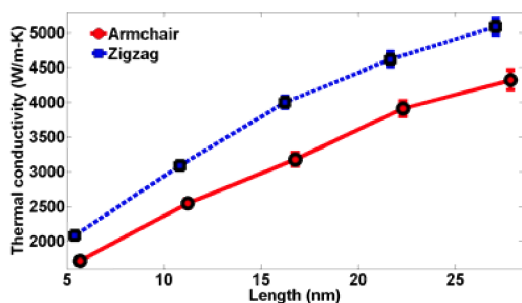
FIGURE 5. Thermal conductivity of rectangular GNRs with armchair (solid line) and zigzag (dashed line) long edges versus their length at 300K.

SUMMARY

In summary, we have used classical molecular dynamics to calculate the thermal conductivity of rectangular GNRs of few nanometers in size. The calculated thermal conductivity, although limited by the size of the GNR, is on the same order of magnitude as the value of experimentally measured for graphene. We showed that the thermal conductivity depends on edge chirality and the zigzag-edged GNRs have larger thermal conductivity than the armchair-edged GNRs. We also studied the size dependence of the thermal conductivity.

ACKNOWLEDGMENTS

REFERENCES

1. A. K. Geim and K. S. Novoselov, *Nature Mater.* **6**, 183 (2007).
2. K. S. Novoselov, A. K. Geim, S. V. Morozov, D. Jiang, Y. Zhang, S. V. Dubonos, I. V. Gregorieva and A. A. Firsov, *Science* **306**, 666 (2004).
3. K. S. Novoselov, A. K. Geim, S. V. Morozov, D. Jiang, M. I. Katsnelson, I. V. Grigorieva, S. V. Dubonos and A. A. Firsov, *Nature* **438**, 197 (2005).
4. Y. Zhang, Y. W. Tan, H. L. Stormer and P. Kim, *Nature* **438**, 201 (2005).
5. A. H. Castro Neto, F. Guinea, N. M. R. Peres, K. S. Novoselov and A. K. Geim, *Rev. Mod. Phys.* **81**, 109 (2009).
6. K. Nakada, M. Fujita, G. Dresselhaus and M. S. Dresselhaus, *Phys. Rev. B* **54**, 17954 (1996).
7. Y. W. Son, M. L. Cohen and S. G. Louie, *Nature* **444**, 347 (2006).
8. M. Y. Han, B. Özyilmaz, Y. Zhang and P. Kim, *Phys. Rev. Lett.* **98**, 206805 (2007).
9. Z. Chen, Y. M. Lin, M. J. Rooks and P. Avouris, *Physica E* **40**, 228 (2007).
10. A. A. Balandin, S. Ghosh, W. Bao, I. Calizo, D. Teweldebrhan, F. Miao and C. N. Lau, *Nano Lett.* **8**, 902 (2008).
11. S. Ghosh, I. Calizo, D. Teweldebrhan, E. P. Pokatilov, D. L. Nika, A. A. Balandin, W. Bao, F. Miao and C. N. Lau, *Appl. Phys. Lett.* **92**, 151911 (2008).
12. P. Kim, L. Shi, A. Majumdar and P. L. McEuen, *Phys. Rev. Lett.* **87**, 215502 (2001).
13. E. Pop, D. Mann, Q. Wang, K. Goodson and H. Dai, *Nano Lett.* **6**, 96 (2006).
14. H. O. Pierson, *Handbook of Carbon, Graphite, Diamonds and Fullerenes: Processing, Properties and Applications,* USA: Noyes Publications, 1995.
15. D. W. Brenner, *Phys. Rev. B* **42**, 9458 (1990).
16. S. J. Nosé, *Chem. Phys.* **81**, 511 (1984).
17. W. G. Hoover, *Phys. Rev. A* **31**, 1695 (1985).
18. G. Wu and B. Li, *Phys. Rev. B* **76**, 085424 (2007).
19. P. H. Hunenberger, *Adv. Polym. Sci.* **173**, 105 (2005).
20. D. L. Nika, S. Glosh, E. P. Pokatilov and A. A. Balandin, Preprint at http://arxiv.org/abs/0904.0607, 2009.